J. Biochem. 2009;146(5)713–723
doi:10.1093/jb/mvp117

Expression, Purification and Characterization of Soluble Recombinant Periostin Protein Produced by *Escherichia coli*

Issei Takayama[1,2], Isao Kii[1] and Akira Kudo[1,*]

[1]Department of Biological Information, Graduate School of Bioscience and Biotechnology; and [2]Global COE Program, Evolving Education and Research Center for Spatio-Temporal Biological Network, Graduate School of Bioscience and Biotechnology, Tokyo Institute of Technology, 4259 Midori-ku, Nagatsuta, Yokohama 226-8501, Japan

Received June 20, 2009; accepted July 11, 2009; published online July 24, 2009

Periostin is a matricellular protein participating in the tissue remodelling of damaged cardiac tissue after acute myocardial infarction and of the periodontal ligament in mice. However, further studies on the periostin protein have been limited by the intrinsic difficulty of purifying this protein produced in *Escherichia coli* due to its insolubility. Here, we demonstrate the expression of recombinant periostin protein with high solubility and monodispersity in *E. coli*. Periostin is composed of an amino-terminal EMI domain, a tandem repeat of 4 fas1 domains (RD1-4), and a carboxyl-terminal region (CTR). We expressed the RD4-CTR region tagged with GST at amino-terminal and 6× Histidine at carboxyl-terminal end in *E. coli*. The recombinant protein was purified by using GSH-Sepharose and nickel chelation affinity chromatography, followed by gel filtration chromatography. The RD4-CTR protein exhibited high solubility and monodispersity. On average, 9.1 mg of purified RD4-CTR was routinely obtained from 1 L of culture media. Furthermore, the RD4-CTR was biochemically active, because it bound to the RD1-4, the same as intact periostin protein that had been purified from mammalian cells. Our results should enable us to produce the periostin recombinant protein in large quantities and facilitate future studies on functional and structural analyses of periostin.

Key words: extracellular matrix, fasciclin I, periodontal ligament, periosteum, periostin.

Abbreviations: GST, glutathione-S-transferase; CBB, Coomassie brilliant blue; HRP, horseradish peroxidase; ECM, extracellular matrix; RD, repeat domain; RD1-4, tandem repeat of 4 fas1 domains; Ni-NTA, nickel chelation affinity chromatography; CTR, carboxyl-terminal region; DMEM, Dulbecco's modified eagle medium; FBS, fetal bovine serum, PBS, phosphate-buffered saline; HA, haemagglutinin; DTT, dithiothreitol; EDTA, ethylenediaminetetraacetic acid.

Mechanical strength of connective tissues depends on the integrity of the extracellular matrix (ECM). ECM components have been regarded not only as mechanical elements, but also as regulators of cellular differentiation (*1*). Integrity of the ECM is based on the framework of a fibronectin matrix, which is required for fibrillogenesis of multiple ECM proteins (*2*). Organization of this fibronectin matrix is described as an integrin-mediated process (*3*). Fibrillogenesis of the ECM takes place in the cell–matrix boundary, known as the matricellular space. Several secreted proteins concentrated in the matricellular space are thought to be involved in ECM fibrillogenesis (*4*) and have been designated as matricellular proteins (*5*).

In this study, we focused on periostin, a matricellular protein of the fasciclin I family of proteins (*6*). Periostin is composed of an amino-terminal EMI domain, tandem repeat of 4 fas1 domains (RD1, RD2, RD3 and RD4), and a carboxyl-terminal region (CTR). Periostin protein was purified from the culture supernatant of the osteoblast cell line MC3T3-E1 and shown to exhibit heparin-binding activity (*7*). The EMI domain is a small module rich in cysteines and found in EMILINs (*8*) and multimerin (*9*), which are glycoproteins of the ECM. This EMI domain has been demonstrated to interact with fibronectin (Kii *et al*., submitted for publication). Fas1 domains are present in many other secreted and membrane-anchored proteins (*10*). Most of these proteins contain multiple Fas1 domains. The crystallographic analysis of Fas1 domains 3–4 of fasciclin I (PDB ID 1o70) and the structural study of MPB70 (PDB ID 1nyo) by NMR showed that the Fas1 domain is a globular domain of an ∼30 Å in a diameter (*11*, *12*). Fas1 domains of βig-h3, a periostin orthologue, have been proposed to be binding sites for integrins (*13–15*). In mammals, periostin is expressed in the dense connective tissues, such as the periosteum, periodontal ligament, aorta and heart valves (*6*, *16*), which tissues are constantly subjected to mechanical strains from physical exercise, mastication and blood flow and pressure, respectively. We and others recently demonstrated that the rate of heart ruptures and death caused by acute cardiac infarction is higher in *periostin*$^{-/-}$ mice than in their wild-type counterparts (*17*, *18*). Periostin plays a

*To whom correspondence should be addressed.
Tel/Fax: +81-45-924-5719, E-mail: akudo@bio.titech.ac.jp

role in the cross-linkage between each collagen fibril, and is involved in collagen fibrillogenesis (*17*, *19*). Furthermore, periostin has been thought to act in cell adhesion, migration and growth *in vitro* (*17*, *20*). Our previous study also showed that periostin is expressed in the capsule around tumours and that the loss of periostin causes impaired capsule formation and progression of tumour growth (*21*). Periostin has been suggested to suppress the invasiveness of bladder cancer (*22*).

The CTR of periostin has received increasing attention because of its regulatory role in the function of periostin (*22*). The CTR has several alternative spliced variant forms (*6*, *23*). In a previous study, we showed that the CTR is constructed by exons a1, a2, b, c1, c2, d, e, f1 and f2, which correspond to exons 15–23 (ENSMUST00000081564: the number in the Ensembl Genome Browser) in the mouse genome. In the infarcted myocardium, the ΔbΔe (deletion of exons b and e) variant form is preferentially detected (*17*). In bladder cancer, the alternatively spliced variant forms display different suppressive activity towards the metastasis of the cancer cells (*23*). Thus, the CTR variant forms possess distinct functions. High production of the CTR variant forms of periostin must be useful for functional and structural assay.

In this study, we demonstrate the expression of the Fas1 domains tagged with 6× Histidine, and of the CTR as a GST fusion protein, in *Escherichia coli*. Furthermore, we also demonstrate the expression of the RD4-CTR tagged with GST at its amino-terminal and 6× Histidine at its carboxyl-terminal end in *E. coli*. The recombinant proteins were purified by using GSH-Sepharose and Ni-NTA resin, followed by gel filtration chromatography. The recombinant RD4-CTR protein exhibited monodispersity when subjected to gel filtration analysis. The recombinant RD4-CTR bound to the full-length periostin and periostin tandem repeat of 4 fas1 domains (RD1-4) that had been purified from the culture supernatant of 293T cells expressing the full-length periostin and the RD1-4. Therefore, we suggest that RD4-CTR is the biochemically active part of the periostin protein that binds to the full-length periostin and the RD1-4, and that the recombinant RD4-CTR protein is suitable for functional and structural analyses of periostin.

MATERIALS AND METHODS

Reagents—All reagents were purchased from Nacalai Tesque Inc. (Kyoto, Japan), unless otherwise specified.

Detection of Alternatively Spliced Variant Forms of the Periostin Transcript in Periodontal Tissues of Mice—To identify the alternatively spliced variant forms of the periostin transcript in periodontal tissues of mice, we performed RT-PCR analysis. Incisors and molars were eviscerated from mandibles and maxillae of 11-week-old C57BL/6 mice by using an electrical grinder, and then were immersed in ISOGEN (Wako Pure Chemical Co., Japan). Care and experiments with animals were in accordance with the guidelines of the animal care and use committees at Tokyo Institute of Technology. Total RNA was extracted from the periodontal tissue surrounding the surface of these incisors and molars. The purified total RNA was subjected to reverse transcription by using a first-strand cDNA synthesis kit (Life Science, St. Petersburg, FL, USA). To detect the alternatively spliced variant forms, we used the specific primers for each variant form, as described previously (*17*). Complementary DNA (cDNA) corresponding to each variant form was amplified with ExTaq DNA polymerase (TAKARA BIO INC., Japan). PCR parameters were as follow: initial denaturation at 95°C for 3 min followed by 26 cycles of denaturation at 95°C for 1 min, and annealing and extension at 68°C for 1 min and a final extension at 72°C for 2 min. The amplified DNA bands were confirmed by performing 15% polyacrylamide gel electrophoresis.

Prediction of the Disorder Region of Mouse Periostin Protein—The disorder region of periostin protein (Accession: Q62009) was predicted by the DISOPRED2 disorder prediction server (*24*) with the default parameters.

Construction of the Expression Vectors—To construct GST-RD fusion proteins, we amplified each RD region from the cloning vector harbouring mouse *periostin* cDNA. The PCR primers for each RD region were as follow: RD1, ACCCAGGATCCGCTGGAAGTTCTGTTCC AGGGGCCCGGCATTGTGGGAGCC (forward) and ACC GAATTCTCATTAAATTTGTGTCAGGAC (reverse); RD2, ACCCAGGATCCGCTGGAAGTTCTGTTCCAGGGGCCC GGTACCTCCATCCAA (forward) and ACCGAATTCTCA TTAAGAATCAGGAATGAG (reverse); RD3, ACCCAGGA TCCGCTGGAAGTTCTGTTCCAGGGGCCCTCTGCCAAA CAAGTT (forward) and ACCGAATTCTCATTATGCTGG TTGGATGAT (reverse); RD4, ACCCAGGATCCGCTG GAAGTTCTGTTCCAGGGGCCCGAGAAATCCCTGCAC (forward) and ACCGAATTCTCATTATGCTGGATAGAG GAG (reverse). Each amplified fragment was digested with EcoRI and BamHI, and then subcloned into pUC119. To produce recombinant CTR(Δb) of periostin in *E. coli*, we changed the rare codons in the CTR(Δb) to synonymous codons to prevent reduction of translation efficiency in the bacteria. We then designed the following primers for the codon exchange: CTR, ACCGGATCCGCA GATATTCCAGTTGGAAATGAT (forward) and ACCGGA TCCGCGGCCGCGGTACCTTATCACTGAGAACGGCCT TCACGTGAGCGACGACGAGGCCCTTGAACACGTTTG TTGGCTGGAATCTTCTTTGCAGGTGTGTC (reverse). The amplified fragment was digested with BamHI, and then subcloned into pUC119. To produce various recombinant RD4-CTR constructs, we designed the following primers: RD4-CTR(Δf), ACCGAATTCGAGAAATCCCTG CACGACAAG (forward) and ACCGGATCCTCATTA TCCCTGAAGCAGTCTTTTAATCTCCTC (reverse); RD4-CTR(ΔeΔf), ACCGAATTCGAGAAATCCCTGCACGAC AAG (forward) and ACCGGATCCTCATTATTGCAAGAA TTTCTGCAAGGTCTC (reverse); RD4-CTR(ΔbΔf), ACCG AATTCGAGAAATCCCTGCACGACAAG (forward) and ACCGGATCCTCATTATCCCTGAAGCAGTCTTTTAATC TCCTC (reverse); and RD4-CTR(ΔbΔeΔf), ACCGAATTC GAGAAATCCCTGCACGACAAG (forward) and ACC GGATCCTCATTATTGCAAGAATTTCTGCAAGGTCTC (reverse). The amplified fragments were digested with EcoRI and BamHI, and then subcloned into pUC119.

To produce recombinant RD4-CTR(ΔbΔeΔf)-His and RD4-His constructs, we designed the following primers: RD4-CTR(ΔbΔeΔf)-His, ACCGAATTCGAGAAATCCCTG CACGACAAG (forward) and ACCGGATCCTCATTAGT GATGGTGATGGTGATGTTGCAAGAATTTCTGCAAGG TCTC (reverse); and RD4-His, ACCGAATTCGAGAAATC CCTGCACGACAAG (forward) and ACCGGATCCTCATT AGTGATGGTGATGGTGATGTGCTGGATAGAGGAGTT TGTCCACG (reverse). The amplified fragments were digested with EcoRI and BamHI, and then subcloned into pBluescript SK+.

Each fragment was amplified with KOD plus DNA polymerase (TOYOBO, Osaka, Japan). PCR parameters were as follow: initial denaturation at 95°C for 3 min followed by 20 cycles of denaturation at 95°C for 1 min, annealing at 50°C, and extension at 68°C for 1 min. The resultant products were subcloned as described above. These samples were sequenced by using a BigDye® Terminator v3.1 Cycle Sequencing Kit and ABI PRISM 3100 Genetic Analyzer (Applied Biosystems, Foster City, CA, USA). After confirmation of the sequences, RD4-CTR(Δf), RD4-CTR(ΔeΔf), RD4-CTR(ΔbΔf) and RD4-CTR (ΔbΔeΔf) were digested with EcoRI and SalI, and subcloned into EcoRI and SalI sites of pGEX6P-1 (GE Healthcare UK Ltd., Buckinghamshire, UK). RD4-CTR (ΔbΔeΔf)-His and RD4-His were digested with EcoRI and NotI, and subcloned into EcoRI and NotI sites of pGEX6P-1 (GE Healthcare). CTR was digested with BamHI and NotI, and subcloned into BamHI and NotI sites of pGEX6P-1. Each Fas1 domain (RD1, RD2, RD3 and RD4) was digested with EcoRI and BamHI, and subcloned into EcoRI and BamHI sites of pET-Duet (Clontech, Palo Alto, CA, USA). The expression vector for periostin(Δb)-flag, which was periostin(Δb) tagged with a flag peptide at its carboxyl-terminal end, was constructed by using standard PCR methods. Briefly, an amplified DNA fragment was subcloned into pUC119. After sequence confirmation, the DNA fragment was subcloned into pCAGIPuro. Full details will be provided upon request. The expression vector for RD1-4-HA was described elsewhere (Kii *et al*., submitted for publication).

Expression and Purification of Recombinant Mouse Periostin in E. coli—Escherichia coli strain Rosetta (DE3) pLysS cells (Novagen, Madison, WI, USA) were transformed with the expression vectors, and cultured in LB media containing 100 mg/l ampicillin and 50 mg/l chloramphenicol. Expression was induced by the addition of 1 mM isopropyl-β-D-thiogalactopyranoside (IPTG), when the culture had reached an OD_{600} of ~0.6. After induction for 20 h at 18°C, the cells were collected by centrifugation at 6000*g* for 5 min, and suspended in cell lysis buffer containing 50 mM Tris–HCl (pH 8.0) and 500 mM NaCl, and then frozen in liquid N_2. After thawing, Triton X-100 (final concentration at 0.1%) was added to cell lysates, which were then incubated at 4°C for 10 min. After gentle sonication of the lysates, $MgCl_2$ (final concentration at 1 mM) and DNase I (final concentration of ~10 μg/ml) were added to the cell lysates, and incubation was continued at 4°C for 20 min. Cell debris and larger particles were removed by centrifugation at 9000 g for 30 min, and the supernatant was then filtered through a 0.45-μm filter.

The supernatant of the cell lysate containing the protein tagged with GST at its amino-terminal and 6× Histidine at its carboxyl-terminal end was applied onto a GSH-Sepharose 4B column (GE Healthcare), which had been pre-equilibrated with 50 mM Tris–HCl (pH 7.0) buffer containing 150 mM NaCl. After excessive washing of the column with the equilibrating buffer, the junction between GST and the recombinant protein was cleaved by the addition of PreScission protease (GE Healthcare) in 50 mM Tris–HCl, containing 150 mM NaCl, 1 mM DTT and 1 mM EDTA to the column. The recombinant protein was then eluted with two column volumes of 50 mm Tris–HCl (pH 7.0) containing 150 mm NaCl. Then, the eluate was loaded onto a pre-equilibrated column of Ni-NTA (Qiagen, Valencia, CA, USA). The protein-bound Ni-NTA resin was washed with PBS containing 20 mM imidazone. The bound proteins were then eluted with PBS containing 200 mM imidazole. The eluate was dialysed against 50 mm Tris–HCl (pH 7.0) containing 500 mm NaCl, and then concentrated by using an Amicon Ultra 15 10K (Millipore, Bedford, MA, USA). The concentrated protein was loaded onto a Superose 6 column (GE Healthcare) to confirm the protein size and monodispersity.

The supernatant of the cell lysate containing the recombinant protein tagged with 6× Histidine was applied to Ni-NTA resin (Qiagen). The pellet containing inclusion bodies of the recombinant protein were solubilized with 8 M urea, and then applied to the Ni-NTA resin. After the resin had been washed with PBS containing 8 M urea and 20 mM imidazole, the 6× Histidine-tagged proteins were eluted with PBS containing 8 M urea and 200 mM imidazole.

To analyse the purity of the recombinant proteins, we performed SDS–PAGE. The protein samples were diluted 1 : 1 with 2× SDS sample loading buffer (0.12 M Tris–HCl, pH 6.8, containing 3.4% SDS, 10% glycerol and 20 mM DTT), heated at 95°C for 5 min and then loaded onto the gels. The proteins were stained with CBB R-250. Purity was estimated from the density of the SDS–PAGE gels using the ImageJ program (NIH). The concentration of the recombinant proteins was determined by using CBB solution for protein assays with BSA as the standard.

Expression and Purification of Recombinant Mouse Periostin from Mammalian Cells—293T cells were grown in DMEM supplemented with 10% FBS (JRH, Japan), 100 U/ml of penicillin, and 100 μg/ml of streptomycin. The cells were transfected with the pCAGIPuro plasmid vectors by using Lipofectamine 2000 (Invitrogen, Carlsbad, CA, USA) according to the manufacturer's instructions. The transfectants stably expressing the recombinant periostin(Δb)-flag or RD1-4-HA proteins were selected in the presence of 4 μg/ml of puromycin. They were then cultured with Opti-MEM (GIBCO, Invitrogen) for 2 days in the confluent condition to secrete the recombinant proteins. The cell culture supernatant was filtered through a 0.45-μm filter, and then loaded onto an anti-flag antibody-conjugated or anti-HA antibody-conjugated agarose chromatography column (Sigma, St. Louis, MO, USA), respectively. The column was washed twice with TBS (150 mM NaCl, 20 mM Tris, pH7.6), and the protein was eluted with 100 mM glycine-HCl (pH 3.0). The eluate was immediately neutralized

with 1 M Tris–HCl (pH 8.0), which had been previously added to the collection tubes. NaCl (final concentration of 200 mM) was added to the solutions. The eluate was dialysed with TBS, and then concentrated by using an Amicon Ultra 4 30K (Millipore, USA). The protein concentration was determined as described above.

Solid-Phase Binding Assay—Ninety-six-well plates (Immulon 2HB, Thermo, Milford, MA, USA) were coated with 10 μg/ml RD4-CTR(ΔbΔeΔf)-His, RD4-His, RD1-4-HA or periostin(Δb)-flag in PBS overnight at 4°C. After discarding of the solutions, the plates were blocked with 5% BSA for 1 h at room temperature. Next, the plates were incubated with RD1-4-HA or periostin(Δb)-flag ligand in PBS for 2 h at room temperature, and washed three times with PBS. The bound RD1-4-HA protein was detected by using anti-HA antibody (Clone DW2, Upstate, Millipore), and the bound periostin-flag protein was detected by using anti-DDDDK-tag antibody (MBL, Nagoya, Japan), followed by incubation with HRP-conjugated anti-rabbit IgG antibody (Southern Biotech, AL, USA). The plates were washed, and then incubated for 20 min with peroxidase substrate *O*-phenylenediamine (0.4 μg/ml) in 50 mM citrate buffer (pH 4.6) containing 0.003% H_2O_2. After the addition of 6N H_2SO_4 to stop the reaction, the absorbance at 490 nm was detected with a Micro Plate Reader (Biorad Model 550).

RESULTS

Identification of Periostin Alternatively Spliced Variant Forms in the Periodontal Tissue of Mice—*Periostin*$^{-/-}$ mice show eruption disturbance of their incisors (*25*), suggesting that periostin is involved in the remodelling of the periodontal tissue. However, it is unclear which alternatively spliced variant form plays a role in the remodelling. To identify the major spliced variant form of periostin in mouse periodontal tissue, we examined the expression pattern of the variant forms in mouse periodontal tissues. We then performed RT-PCR analysis by using three combinations of specific primers for detecting each alternatively spliced variant form (Fig. 1A). We detected four alternatively spliced variant forms, *i.e*. full (full-length), Δb (deletion of exon b), Δe (deletion of exon e) and ΔbΔe (deletion of exons b and e). One specific spliced form, ΔbΔe, was dominantly detected as the lowest electrophoretic band (Fig. 1A, arrowhead). This expression pattern is consistent with the previously reported one found in acute myocardial infarcts at the initial stage (*17*). Thus, these results demonstrate that the ΔbΔe spliced variant form of periostin is dominantly expressed in mouse periodontal tissues.

Prediction of the Disordered Region in Mouse Periostin Protein—To produce the recombinant periostin protein, we designed an expression construct optimized for expression in *E. coli*, because the disordered region might affect protein stability and purification efficiency (*24*). To find the disordered region of full-length periostin, we used the DISOPRED2 server. The disorder profile plot is shown in Fig. 1B. The 185–191 amino acid region, corresponding to the RD1, and the 822–838 one, corresponding to exon f2, were predicted to be disordered. We then removed the carboxyl-terminal amino acid residues of the periostin sequence until the DISOPRED2 did not output the disordered region. Finally, exons f1 and f2 were predicted to be the disordered region (data not shown). These results suggest that the RD1 and exon f2 which contains the heparin-binding motif are probably flexible and are not suitable for protein production.

Screening for a Soluble Recombinant Periostin Protein—To obtain the soluble recombinant periostin protein in *E. coli*, we generated expression vectors for each Fas1 domain and CTR except for the EMI domain; because it is thought to be difficult to obtain a soluble EMI domain, as it contains six conserved cysteine residues. Eukaryotic proteins that contain many cysteine residues tend to be misfolded in *E. coli* (*26*). We first purified soluble and insoluble RD recombinant proteins, which were fused with 6× Histidine at their amino acid terminus, by using Ni-NTA resin. The purified proteins were analysed by SDS–PAGE, and stained with CBB (Fig. 1C). The RD4 showed the highest solubility among the RDs (Fig. 1C). RD2 showed relatively high solubility (Fig. 1C); however, the RD1 and RD3 formed inclusion bodies. The insoluble pellet of the RDs was solubilized with 8 M Urea, and purified with Ni-NTA resin, indicating that the RDs could be purified in the denatured condition. These data suggested RD2 and RD4 to be possible candidates of the soluble protein.

We next generated an expression vector for CTR(Δb). The CTR(Δb) contains rare codons for *E. coli* in its 3′ region (data not shown). Therefore, by using PCR-based site-directed mutagenesis, we exchanged these rare codons for synonymous codons to prevent reduction of translation efficiency in *E. coli*. To produce the CTR(Δb) in the bacteria, we generated an expression vector for the GST fusion protein of CTR(Δb). The GST-CTR(Δb) was expressed at a high level in *E. coli*, and exhibited high solubility. Soluble GST-CTR(Δb) was loaded onto a GSH-Sepharose column. The CTR(Δb) was eluted from the GSH-Sepharose by PreScission protease-mediated cleavage between GST and CTR(Δb). CTR(Δb) showed high solubility (Fig. 1D), suggesting it to be a possible candidate of the soluble protein.

RD4-CTR(ΔbΔeΔf) Construct Showed High Solubility and Monodispersity—We performed large-scale protein expression in *E. coli*. We constructed the GST-RD4-His expression vector, in which the RD4 was fused with GST at its amino-terminal and 6× Histidine at its carboxyl-terminal end (Fig. 2A). Tandem purification with GSH-Sepharose and Ni-NTA was performed. The GST-RD4-His was expressed at a high level with high solubility. The purification result is shown in Fig. 2B. The RD4-His exhibited monodispersity in the gel filtration chromatography (Fig. 2C and D). We estimated the yield of the RD4-His to be 5.5 mg/l of LB culture (Table 1).

Although the CTR(Δb) was expressed at a high level, it did not exhibit monodispersity in the gel filtration chromatography (data not shown), suggesting that CTR(Δb) would be inappropriate for the functional analysis. We then focused on the disordered region of the CTR, and generated the CTR(ΔbΔeΔf) expression vector. However, the CTR(ΔbΔeΔf) was expressed at

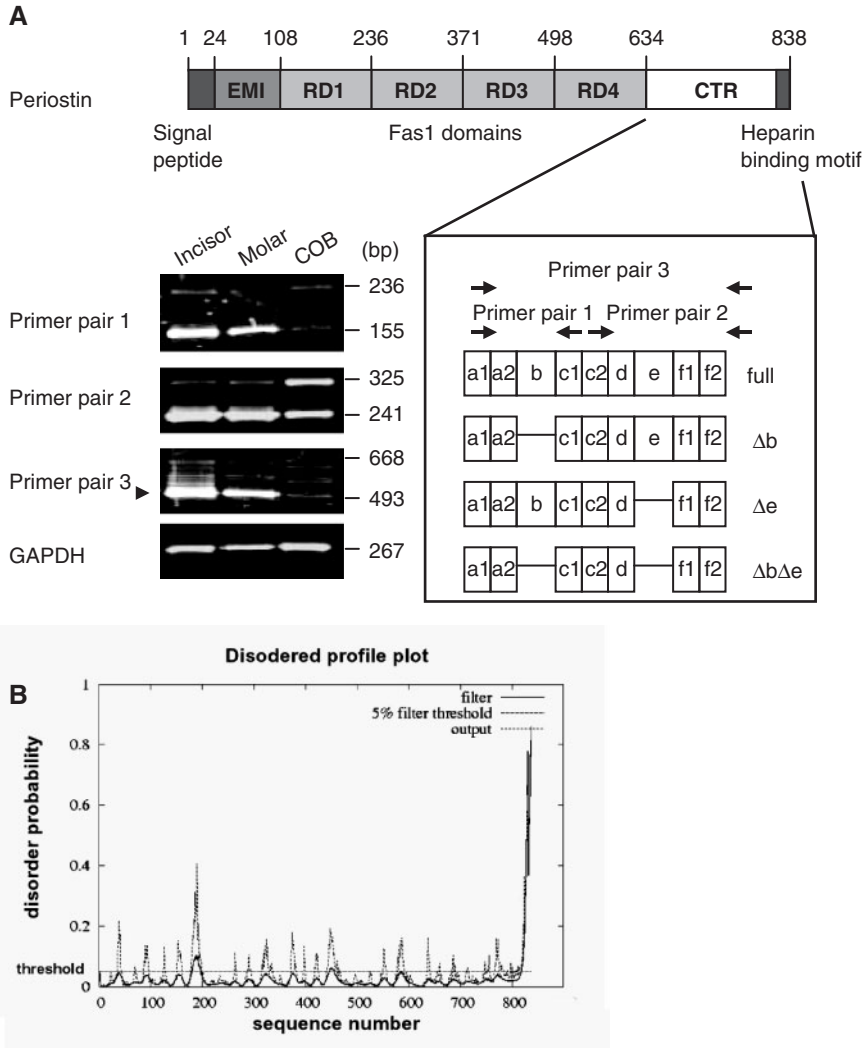

Fig. 1. **Expression of recombinant periostin proteins in *E. coli*.** (A) Expression profile of the alternatively spliced variant forms of periostin in the periodontal tissue of incisors and molars from 11-week-old C57BL/6 mice and in primary calvarial osteoblasts (COB). Schematic view of the periostin protein is shown: signal peptide, the EMI domain, the RD1-4 and the CTR. The heparin-binding motif, corresponding to exon f2, is indicated at the carboxyl-terminal end of the CTR. The PCR primer pairs for the detection of the spliced variant forms are shown in the rectangular box. Periostin ΔbΔe is indicated by the arrowhead. GAPDH is shown as an internal control. (B) Disorder profile of periostin protein. The plot shows the position in the sequence having probability of disorder. The DISOPRED2 server predicted the disordered region of periostin (full length) to be in 185–191 and 822–838 amino acid regions, which correspond to the RD1 and the heparin-binding motif, respectively, at the default threshold. (C) Expression and purification of the recombinant RDs (RD1, RD2, RD3 and RD4) in soluble and insoluble fractions prepared from *E. coli*. The RDs were expressed as amino-terminal 6× Histidine-tagged proteins. Insoluble protein was solubilized in 8 M urea. Samples were purified by using Ni-NTA chromatography. Arrowheads indicate the recombinant RDs. SM, size marker. (D) Expression and purification of the recombinant CTR of periostin produced by *E. coli*. The CTR was expressed as an amino-terminal GST-tagged protein, and purified by using GSH-Sepharose chromatography. The CTR was eluted by PreScission protease-mediated cleavage between the GST tag and the CTR.

a low level, and became an inclusion body (data not shown). Hence, we next focused on the monodispersity of the RD4-His. GST-RD4-CTR(Δb) was expressed in a large amount with high solubility; however, RD4-CTR(Δb) did not exhibit monodispersity (data not shown). Therefore we focused on the disordered region of the CTR, and constructed the GST-RD4-CTR (ΔbΔeΔf)-His expression vector, in which the exons of b, e, f1 and f2 in the CTR were deleted and the truncated protein was fused with GST at its amino-terminal and 6× Histidine at its carboxyl-terminal end (Fig. 3A). Tandem purification with GSH-Sepharose and Ni-NTA was performed. The GST-RD4-CTR(ΔbΔeΔf)-His was expressed at a high level with high solubility (Fig. 3B). The RD4-CTR(ΔbΔeΔf)-His exhibited monodispersity in the gel filtration chromatography (Fig. 3C and D). We estimated the yield of the RD4-CTR(ΔbΔeΔf)-His to be 9.1 mg/l of LB culture (Table 2). To eliminate the effect of 6× Histidine tag, we constructed the recombinant expression vector without the 6× Histidine tag.

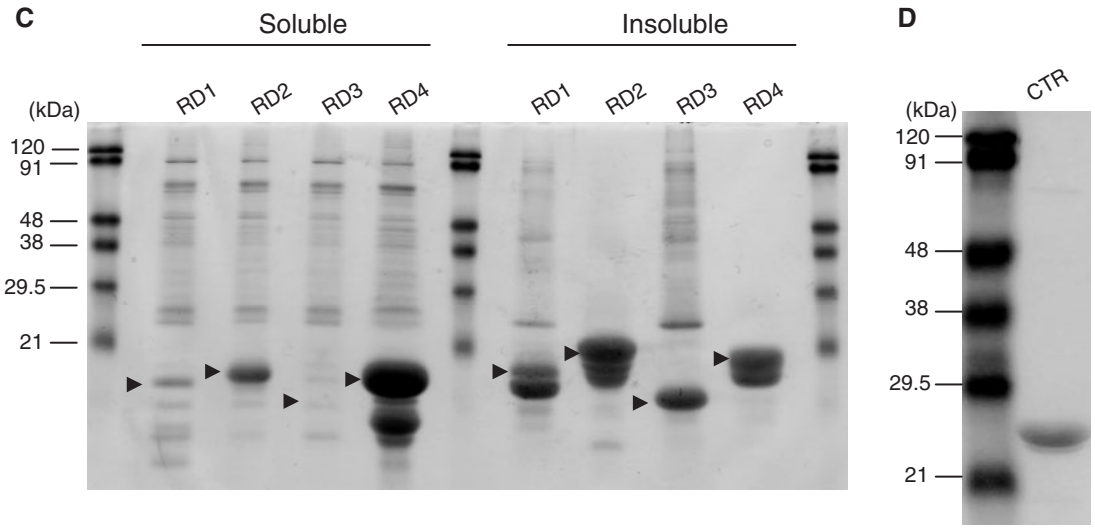

Fig. 1. Continued.

The GST-RD4-CTR(ΔbΔeΔf) was also expressed at high levels with high solubility, and the RD4-CTR (ΔbΔeΔf) exhibited monodispersity in the gel filtration chromatography (data not shown). We also confirmed monodispersity of the other spliced variants of CTR: RD4-CTR(Δf), RD4-CTR(ΔbΔf) and RD4-CTR(ΔeΔf) (data not shown). These results indicated RD4-CTR (ΔbΔeΔf)-His to be appropriate for the functional analysis of the CTR.

RD4-CTR(ΔbΔeΔf)-His Bound to the RD1-4 of Periostin—A solid-phase binding assay was performed to determine the activity of the recombinant periostin proteins. An earlier report demonstrated that periostin binds to itself in a homophilic manner (*27*). This report also suggested that the RD1-4 could bind to each other. Thus, we could characterize the periostin protein activity in terms of the homophilic binding of RD1-4. We first generated an RD1-4 expression vector. However, the RD1-4 was expressed at a low level, and became an inclusion body in *E. coli* (data not shown). As we were aware of a report indicating that recombinant periostin protein could be purified from eukaryotic cells (*27*), we then generated the pCAGIPuro RD1-4-HA expression vector, transfected mammalian cells with it and obtained a stable 293T transfectant. We purified the recombinant RD1-4-HA, which was fused with HA peptide at its carboxyl-terminal end, from the cell culture supernatant of 293T cells expressing RD1-4-HA. A schematic view of the RD1-4-HA construct is shown in Fig. 4A. Anti-HA antibody-conjugated agarose resin was used for purification of RD1-4-HA. The purified recombinant proteins were analysed by SDS–PAGE, and stained with CBB (Fig. 4B and Table 3). To obtain a positive control, we also generated the pCAGIPuro periostin(Δb)-flag, which was fused with a flag peptide at its carboxyl-terminal end, and purified periostin(Δb)-flag from the cell culture supernatant of 293T cells by using anti-flag M2 antibody-conjugated agarose resin (Fig. 4A and B and Table 4). These recombinant proteins were used in the solid-phase binding assay.

To evaluate the RD4-CTR(ΔbΔeΔf)-His produced in *E. coli*, we examined the binding of the RD1-4-HA to the RD4-CTR(ΔbΔeΔf)-His. Compared with the BSA-coated negative control plates, the RD1-4-HA bound to the RD4-CTR(ΔbΔeΔf)-His-coated plates in a dose-dependent manner (Fig. 4C), as well as to the periostin(Δb)-flag-coated plates (Fig. 4C), indicating that the RD4-CTR(ΔbΔeΔf)-His exhibited similar binding activity to the RD1-4-HA as the periostin(Δb)-flag protein produced in mammalian cells. However, the RD1-4-HA did not bind to the RD4-His-coated plates (Fig. 4C). To further evaluate the binding activity of the RD4-CTR(ΔbΔeΔf)-His, we examined the binding of periostin(Δb)-flag to the RD4-CTR(ΔbΔeΔf)-His coated on the plate, to the RD4-His, and to the RD1-4-HA. The RD4-CTR(ΔbΔeΔf)-His and the RD1-4-HA bound to periostin(Δb)-flag (Fig. 4D). The RD4-His bound to periostin(Δb)-flag; however, the binding activity was lower than that of the RD4-CTR(ΔbΔeΔf)-His and the RD1-4-HA (Fig. 4D). These data suggest that the RD4-CTR(ΔbΔeΔf)-His exhibits the similar biochemical activity to intact periostin protein produced in mammalian cells.

DISCUSSION

In this study, we demonstrated the expression of the recombinant periostin protein that exhibits high solubility and monodispersity. We modified and improved the production system of the recombinant periostin proteins in *E. coli*, especially, the RD4-CTR(ΔbΔeΔf)-His showed high solubility and monodispersity. From 1l of LB culture, ~9.1 mg of the RD4-CTR(ΔbΔeΔf)-His was obtained. In addition, we found that the purified RD4-CTR(ΔbΔeΔf)-His was biochemically active; because it exhibited binding activity towards RD1-4 similar to that of periostin protein produced in mammalian cells. Furthermore, RD4-His did not exhibit binding activity towards RD1-4, suggesting that the CTR(ΔbΔeΔf) sequence plays a role in this interaction.

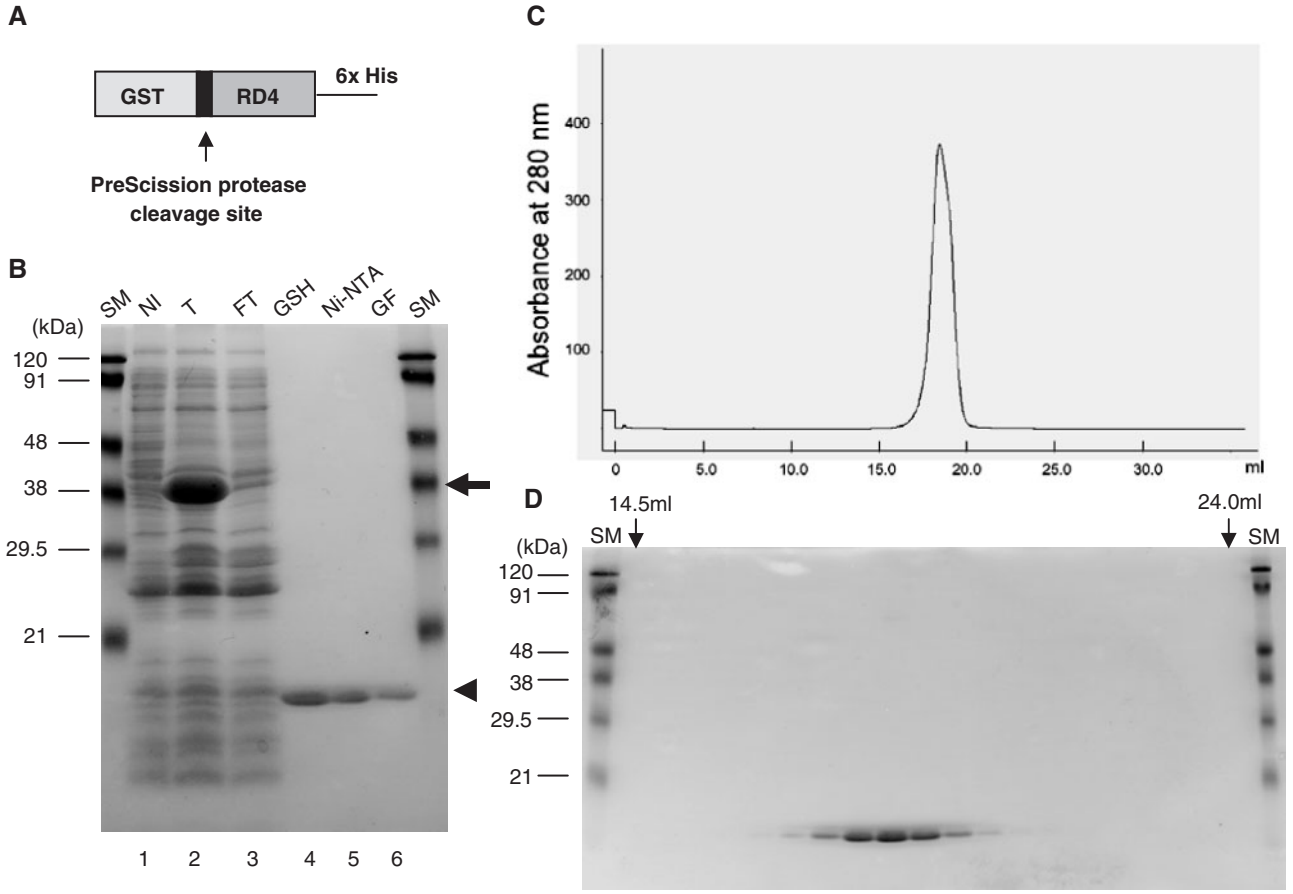

Fig. 2. **Expression in and purification of RD4-His from *E. coli*.** (A) Schematic view of GST-RD4-His. (B) Purity of the recombinant protein was analysed by SDS–PAGE and CBB staining. The GST-RD4-His was purified by a tandem purification protocol using GSH-Sepharose followed by Ni-NTA chromatography. The RD4-His was eluted by PreScission protease-mediated cleavage between GST tag and the RD4-His. Lane 1: total cell lysate from *E. coli* cultured without IPTG (NI); lane 2: total cell lysate from *E. coli* cultured with IPTG (T); lane 3: flow-through fraction of the GSH-Sepharose column (FT); lane 4: protein eluted from the GSH-Sepharose column (GSH); lane 5: protein eluted from the Ni-NTA resin (Ni-NTA); and lane 6: protein purified by gel filtration chromatography (GF). The arrow indicates the recombinant GST-RD4-His; and the arrowhead, the recombinant RD4-His. Size markers (SM) are shown on either side of the gel. (C) FPLC elution profile of the recombinant RD4-His from the Superose 6 gel filtration column. Elution was carried out at a flow rate of 0.4 ml/min. Absorbance at 280 nm was monitored, and 0.5-ml fractions were collected. (D) The fractions eluted from the gel filtration chromatography column were confirmed to contain the recombinant RD4-His proteins by SDS–PAGE followed by CBB staining. Elution volumes are indicated at 14.5 ml and 24.0 ml.

Table 1. **Yield of RD4-His.**

Purification step[a]	Total protein (mg/l)[b]	% of total protein[c]
Step1: Glutathione Sepharose	14.1	97.2
Step2: Ni-NTA resin	10.1	95.2
Step3: Gel filtration	5.50	92.5

[a]The recombinant protein was purified by using GSH-Sepharose. The eluate from the GSH-Sepharose was applied into nickel chelation affinity chromatography, which was then followed by gel filtration chromatography. [b]From CBB Solution for Protein Assay. The unit milligram per litre indicates the yields of recombinant periostin protein from 1 l of LB culture. [c]From gel scanning and digitization.

The DISOPRED2 prediction showed that exons f1 and f2 are the disordered regions, indicating that the peptide regions corresponding to exons f1 and f2 are dynamically flexible and distinct from the regular secondary structure. The deletion of exons f1 and f2 improved the monodispersity of the recombinant periostin protein, indicating that the flexibility of these regions may have affected the stability of the protein folding. Exon f2 encodes the heparin-binding motif of periostin, which is rich in arginine (RRRSR in mouse periostin). It is possible that this cationic region randomly interacts with the anionic surface of the recombinant protein. The RD4-CTR(Δf), the RD4-CTR(ΔbΔf), the RD4-CTR(ΔeΔf) and RD4-CTR(ΔbΔeΔf) showed high solubility and monodispersity, indicating that the monodispersity of RD4-CTR is not affected by the exon b and/or exon e, which can be deleted by the alternative splicing events. The DISOPRED2 prediction also showed that the RD1 contained a disordered region, which is consistent with the insolubility of the RD1 recombinant protein produced in *E. coli*.

The RD4 recombinant protein exhibited extremely high solubility and monodispersity, compared with the

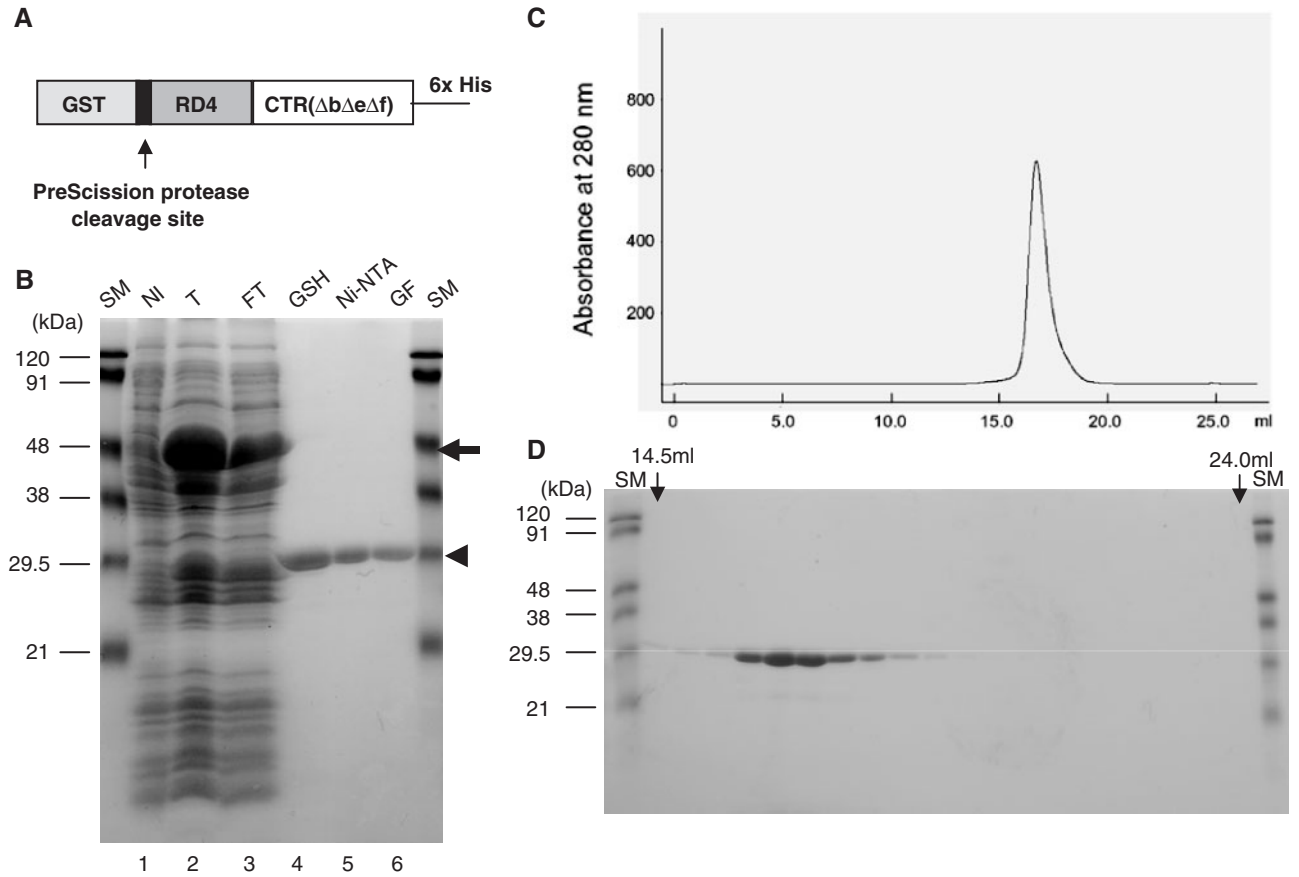

Fig. 3. **Expression in and purification of the recombinant RD4-CTR(ΔbΔeΔf)-His from *E. coli*.** (A) Schematic view of GST-RD4-CTR(ΔbΔeΔf)-His. (B) Purity of the recombinant proteins was analysed by SDS–PAGE and CBB staining. The GST-RD4-CTR(ΔbΔeΔf)-His was purified by the tandem purification protocol using GSH-Sepharose followed by Ni-NTA chromatography. The RD4-CTR(ΔbΔeΔf)-His was eluted by PreScission protease-mediated cleavage between GST tag and the RD4-CTR(ΔbΔeΔf)-His. Lane 1: total cell lysate from *E. coli* cultured without IPTG (NI); lane 2: total cell lysate from *E. coli* cultured with IPTG (T); lane 3: flow-through fraction of the GSH-Sepharose column (FT); lane 4: protein eluted from the GSH-Sepharose column (GSH); lane 5: protein from the Ni-NTA resin (Ni-NTA); and lane 6: protein purified by gel filtration chromatography (GF). The arrow indicates the recombinant GST-RD4-CTR(ΔbΔeΔf)-His; and the arrowhead, the recombinant RD4-CTR(ΔbΔeΔf)-His. (C) FPLC elution profile of the recombinant RD4-CTR(ΔbΔeΔf)-His from the Superose 6 gel filtration column. Elution was carried out at a flow rate of 0.4 ml/min. Absorbance at 280 nm was monitored, and 0.5-ml fractions were collected. (D) The fractions eluted from the gel filtration chromatography column were confirmed to contain the recombinant RD4-CTR(ΔbΔeΔf)-His by SDS–PAGE followed by CBB staining. Elution volumes are indicated at 14.5 ml and 24.0 ml.

Table 2. **Yield of RD4-CTR(ΔbΔeΔf)-His.**

Purification step[a]	Total protein (mg/l)[b]	% of total protein[c]
Step1: Glutathione Sepharose	21.5	94.0
Step2: Ni-NTA resin	11.9	95.2
Step3: Gel filtration	9.10	94.1

[a]The recombinant protein was purified by using GSH-Sepharose. The eluate from the GSH-Sepharose was applied into nickel chelation affinity chromatography, which was then followed by gel filtration chromatography. [b]From CBB Solution for Protein Assay. The unit milligram per litre indicates the yields of recombinant periostin protein from 1 l of LB culture. [c]From gel scanning and digitization.

other RDs. The RD4 recombinant protein of βig-h3, which is an orthologue of periostin, was crystallized (*28*). Furthermore, structure of the RD4 of βig-h3 was also analyzed by NMR analysis, and is available in the PDB (PDB ID 1X3B). The RD3-4 region of *Drosophila* fasciclin I was crystallized, and the crystal structure of it was determined (*11*). Consequently, the RD4 region of the fasciclin I family may be appropriate for the structural analysis. Although the RD2 recombinant protein was soluble, the RD1 and RD3 recombinant proteins showed little solubility. To obtain the soluble RD1 and RD3 proteins, we performed gradual dialysis of the denatured RD1 and RD3 proteins against 8 M to 0 M urea; however, we failed to refold the denatured RD1 and RD3 proteins (data not shown). It is unknown why the RD1 and RD3 proteins are insoluble, compared with the RD2 and RD4 proteins, despite the fact that the RDs share a similar amino acid sequence. Further investigation is necessary to elucidate the insolubility of the RD1 and RD3 proteins produced in *E. coli*.

The solid-phase binding assay showed that the RD1-4-HA bound to periostin(Δb)-flag, which is consistent with

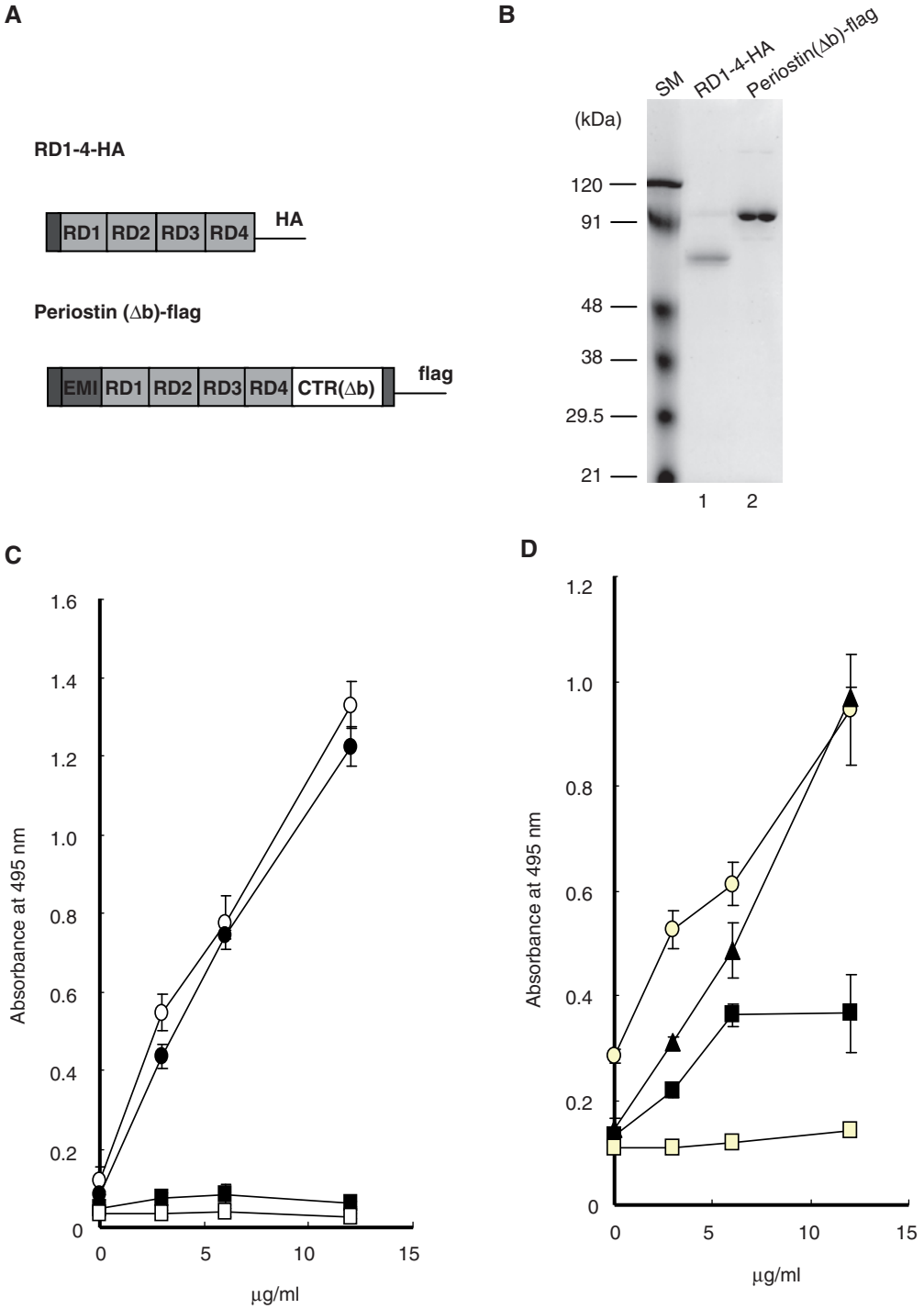

Fig. 4. **Solid-phase binding assay to detect the binding between the recombinant RD4-CTR(ΔbΔeΔf)-His and the RD1-4 of periostin.** (A) Schematic views of RD1-4-HA and periostin(Δb)-flag. (B) Expression in and purification of the RD1-4-HA and periostin(Δb)-flag from mammalian 293T cells. The RD1-4-HA and periostin(Δb)-flag were purified from 293T cells stably expressing RD1-4-HA and periostin(Δb)-flag, respectively. Purification was performed by using anti-HA antibody-conjugated and anti-flag antibody-conjugated agarose, respectively. Eluted proteins were analysed by SDS–PAGE and CBB staining. Lane 1: RD1-4-HA. Lane 2: periostin(Δb)-flag. (C) Binding of the indicated concentrations of RD1-4-HA to periostin(Δb)-flag (closed circle), to recombinant RD4-CTR(ΔbΔeΔf)-His (open circle), to recombinant RD4-His (closed square), and to BSA (open square). The periostin(Δb)-flag, RD4-CTR(ΔbΔeΔf)-His, and RD4-His proteins were coated onto wells of the microtitre plate at 10 μg/ml, and then blocked with BSA. Binding of the RD1-4-HA was performed at room temperature for 2 h. The bound RD1-4-HA was detected with anti-HA antibody, followed by HRP-conjugated secondary antibody. Error bars represent the mean ± SEM. (D) Binding of the indicated concentrations of periostin(Δb)-flag to RD1-4-HA coated on the plate (closed triangle), to recombinant RD4-CTR(ΔbΔeΔf)-His (open circle), to recombinant RD4-His (closed square), and to BSA (open square). Error bars represent the mean ± SEM.

Table 3. **Yield of RD1-4-HA.**

Purification step[a]	Total protein (mg/l)[b]	% of total protein[c]
anti-HA antibody-conjugated agarose	0.472	88.7

[a]The recombinant protein was purified by using anti-HA antibody-conjugated agarose chromatography column. [b]From CBB Solution for Protein Assay. The unit milligram per litre indicates the yields of recombinant periostin protein from 1 l of the cell culture supernatant. [c]From gel scanning and digitization.

Table 4. **Yield of periostin(Δb)-flag.**

Purification step[a]	Total protein (mg/l)[b]	% of total protein[c]
anti-flag antibody-conjugated agarose	1.95	92.5

[a]The recombinant protein was purified by using anti-flag antibody-conjugated agarose chromatography column. [b]From CBB Solution for Protein Assay. The unit milligram per litre indicates the yields of recombinant periostin protein from 1 l of the cell culture supernatant. [c]From gel scanning and digitization.

the earlier report on the homophilic interaction between periostin proteins (*27*), suggesting that the 4 Fas1 domains (RD1-4) is involved in the homophilic interaction. The present study also showed that the RD4-His did not bind to the RD1-4-HA, and weakly bound to periostin(Δb)-flag, suggesting that the RD1-3 appears to be possibly involved in the homophilic interaction. The earlier study showed that the binding of a CTR truncated periostin (periostin-ΔCTR) to both full-length periostin and periostin-ΔCTR was stronger than that of the full-length form, suggesting that the CTR inhibits the intermolecular binding of periostin through the Fas1 domains. The present study revealed that the RD4-CTR(ΔbΔeΔf)-His bound to the RD1-4-HA, indicating that the CTR interacts with the RD1-4. These results suggest that periostin may form an intramolecular interaction between the CTR and the RD1-4, and that the intramolecular interaction may inhibit the homophilic interaction. Moreover, we have demonstrated that the CTR inhibits the interaction between RD1-4 and tenascin-C (Kii *et al*., submitted for publication), possibly indicating that the interaction between the CTR and the Fas1 domains modulates the function of periostin. As we failed to produce the recombinant CTR protein in monodisperse form, further improvement of the production of the CTR in *E. coli* is necessary to elucidate whether the CTR binds to the Fas1 domains.

Our study provides soluble and biologically active recombinant proteins of the alternatively spliced variant forms of periostin, *i.e*. RD4-CTR(ΔbΔeΔf), RD4-CTR(ΔbΔf), RD4-CTR(ΔeΔf) and RD4-CTR(Δf). We believe that these experimental conditions for generating the recombinant periostin proteins should be useful in facilitating future investigations of the functional significance of periostin in cancer progression and acute myocardial infarction. These recombinant proteins exhibited monodispersity. As high solubility and monodispersity of a recombinant protein are required for protein crystallization or NMR analysis, these RD4-CTR variant forms may be useful for structural analysis.

FUNDING

Grants-in-aid (to A.K.) for scientific research from the Ministry of Education, Science, Culture, and Sports of Japan.

CONFLICT OF INTEREST

None declared.

REFERENCES

1. Berrier, A.L. and Yamada, K.M. (2007) Cell-matrix adhesion. *J. Cell Physiol.* **213**, 565–573
2. Pankov, R. and Yamada, K.M. (2002) Fibronectin at a glance. *J. Cell Sci.* **115**, 3861–3863
3. Mao, Y. and Schwarzbauer, J.E. (2005) Stimulatory effects of a three-dimensional microenvironment on cell-mediated fibronectin fibrillogenesis. *J. Cell Sci.* **118**, 4427–4436
4. Bradshaw, A.D., Graves, D.C., Motamed, K., and Sage, E.H. (2003) SPARC-null mice exhibit increased adiposity without significant differences in overall body weight. *Proc. Natl Acad. Sci. USA* **100**, 6045–6050
5. Bornstein, P. (2000) Matricellular proteins: an overview. *Matrix Biol.* **19**, 555–556
6. Horiuchi, K., Amizuka, N., Takeshita, S., Takamatsu, H., Katsuura, M., Ozawa, H., Toyama, Y., Bonewald, L.F., and Kudo, A. (1999) Identification and characterization of a novel protein, periostin, with restricted expression to periosteum and periodontal ligament and increased expression by transforming growth factor beta. *J. Bone Miner. Res.* **14**, 1239–1249
7. Sugiura, T., Takamatsu, H., Kudo, A., and Amann, E. (1995) Expression and characterization of murine osteoblast-specific factor 2 (OSF-2) in a baculovirus expression system. *Protein Expr. Purif.* **6**, 305–311
8. Doliana, R., Bot, S., Bonaldo, P., and Colombatti, A. (2000) EMI, a novel cysteine-rich domain of EMILINs and other extracellular proteins, interacts with the gC1q domains and participates in multimerization. *FEBS Lett.* **484**, 164–168
9. Braghetta, P., Ferrari, A., De Gemmis, P., Zanetti, M., Volpin, D., Bonaldo, P., and Bressan, G.M. (2004) Overlapping, complementary and site-specific expression pattern of genes of the EMILIN/Multimerin family. *Matrix Biol.* **22**, 549–556
10. Zinn, K., McAllister, L., and Goodman, C.S. (1988) Sequence analysis and neuronal expression of fasciclin I in grasshopper and Drosophila. *Cell* **53**, 577–587
11. Clout, N.J., Tisi, D., and Hohenester, E. (2003) Novel fold revealed by the structure of a FAS1 domain pair from the insect cell adhesion molecule fasciclin I. *Structure* **11**, 197–203
12. Carr, M.D., Bloemink, M.J., Dentten, E., Whelan, A.O., Gordon, S.V., Kelly, G., Frenkiel, T.A., Hewinson, R.G., and Williamson, R.A. (2003) Solution structure of the Mycobacterium tuberculosis complex protein MPB70: from tuberculosis pathogenesis to inherited human corneal desease. *J. Biol. Chem.* **278**, 43736–43743
13. Kim, J.-E., Kim, S.-J., Lee, B.-H., Park, R.-W., Kim, K.-S., and Kim, I.-S. (2000) Identification of motifs for cell adhesion within the repeated domains of transforming growth factor-beta-induced gene, beta ig-h3. *J. Biol. Chem.* **275**, 30907–30915
14. Kim, J.-E., Jeong, H.-W., Nam, J.-O., Lee, B.-H., Choi, J.-Y., Park, R.-W., Park, J.Y., and Kim, I.-S. (2002) Identification of motifs in the fasciclin domains of the transforming growth factor-beta -induced matrix protein beta ig-h3 that interact

with the alpha vbeta 5 integrin. *J. Biol. Chem.* **277**, 46159–46165
15. Park, S.J., Park, S., Ahn, H.C., Kim, I.S., and Lee, B.J. (2004) Conformational resemblance between the structures of integrin-activating pentapetides derived from betaig-h3 and RGD peptide analogues in a membrane environment. *Peptides* **25**, 199–205
16. Wang, D., Oparil, S., Feng, J.A., Li, P., Perry, G., Chen, L.B., Dai, M., John, S.W., and Chen, Y.F. (2003) Effects of pressure overload on extracellular matrix expression in the heart of the atrial natriuretic peptide-null mouse. *Hypertension* **42**, 88–95
17. Shimazaki, M., Nakamura, K., Kii, I., Kashima, T., Amizuka, N., Li, M., Saito, M., Fukuda, K., Nishiyama, T., Kitajima, S., Saga, Y., Fukayama, M., Sata, M., and Kudo, A. (2008) Periostin is essential for cardiac healing after acute myocardial infarction. *J. Exp. Med.* **205**, 295–303
18. Oka, T., Xu, J., Kaiser, R.A., Melendez, J., Hambleton, M., Sargent, M.A., Lorts, A., Brunskill, E.W., Dorn, G.W. II, Conway, S.J., Aronow, B.J., Robbins, J., and Molkentin, J.D. (2007) Genetic manipulation of periostin expression reveals a role in cardiac hypertrophy and ventricular remodeling. *Circ. Res.* **101**, 313–321
19. Norris, R.A., Damon, B., Mironov, V., Kasyanov, V., Ramamurthi, A., Moreno-Rodriguez, R., Trusk, T., Potts, J.D., Goodwin, R.L., Davis, J., Hoffman, S., Wen, X., Sugi, Y., Kern, C.B., Mjaatvedt, C.H., Turner, D.K., Oka, T., Conway, S.J., Molkentin, J.D., Forgacs, G., and Markwald, R.R. (2007) Periostin regulates collagen fibrillogenesis and the biomechanical properties of connective tissues. *J. Cell. Biochem.* **101**, 695–711
20. Kuhn, B., del Monte, F., Hajjar, R.J., Chang, Y.S., Lebeche, D., Arab, S., and Keating, M.T. (2007) Periostin induces proliferation of differentiated cardiomyocytes and promotes cardiac repair. *Nat. Med.* **13**, 962–969
21. Shimazaki, M. and Kudo, A. (2008) Impaired capsule formation of tumors in periostin-null mice. *Biochem. Biophys. Res. Commun.* **367**, 736–742
22. Kim, C.J., Yoshioka, N., Tambe, Y., Kushima, R., Okada, Y., and Inoue, H. (2005) Periostin is down-regulated in high grade human bladder cancers and suppresses in vitro cell invasiveness and in vivo metastasis of cancer cells. *Int. J. Cancer* **117**, 51–58
23. Kim, C.J., Isono, T., Tambe, Y., Chano, T., Okabe, H., Okada, Y., and Inoue, H. (2008) Role of alternative splicing of periostin in human bladder carcinogenesis. *Int. J. Oncol.* **32**, 161–169
24. Ward, J.J., McGuffin, L.J., Bryson, K., Buxton, B.F., and Jones, D.T. (2004) The DISOPRED server for the prediction of protein disorder. *Bioinformatics* **20**, 2138–2139
25. Kii, I., Amizuka, N., Minqi, L., Kitajima, S., Saga, Y., and Kudo, A. (2006) Periostin is an extracellular matrix protein required for eruption of incisors in mice. *Biochem. Biophys. Res. Commun.* **342**, 766–772
26. Whitford, D. (2005) Protein expression, purification and characterization in *Proteins Structure and Function*, p. 314, John Wiley and Sons Ltd, West Sussex, England
27. Takayama, G., Arima, K., Kanaji, T., Toda, S., Tanaka, H., Shoji, S., McKenzie, A.N., Nagai, H., Hotokebuchi, T., and Izuhara, K. (2006) Periostin: a novel component of subepithelial fibrosis of bronchial asthma downstream of IL-4 and IL-13 signals. *J. Allergy Clin. Immunol.* **118**, 98–104
28. Yoo, J.H., Kim, E., Kim, J., and Cho, H.S. (2007) Crystallization and preliminary crystallographic analysis of the fourth FAS1 domain of human BigH3. *Acta Crystallogr. Sect. F Struct. Biol. Cryst. Commun.* **63**, 893–895